International Journal Publishing
INFLUENCE: International Journal of Science Review
Volume 8, No. 3, 2026
https://influence-journal.com/index.php/influence/index

Theoretical Design of a Belt Sander Wood Sanding Machine for Small-Scale Industries

Candra Prayoga Aditama Paputungan[1], Herotje Siwi[2]
[1,2]Politeknik Negeri Manado, Indonesia
Email: candrapapputungan@gmail.com

Abstract. Manual wood sanding in small workshops requires considerable time and labor but may produce inconsistent surface quality. This study aimed to develop a theoretical design for a belt-sander wood sanding machine and determine the specifications of its main components. An engineering design approach was used, comprising a literature review, identification of design requirements, component selection, preparation of two- and three-dimensional AutoCAD drawings, and analytical calculations for the motor, pulley and V-belt transmission, rollers, shaft, and frame. The proposed machine uses a 1 HP (0.746 kW), 1390 rpm electric motor, 80 mm driving and 120 mm driven pulleys, an A-type V-belt, 100 mm rollers, a 25 mm S45C shaft, UCP205 bearings, and a 40 × 40 × 2 mm hollow-steel frame. The calculations yielded a drive-roller speed of 926.67 rpm, motor torque of 5.13 N·m, theoretical roller torque of 7.70 N·m, sanding-belt speed of 4.85 m/s, tangential force of 154 N, theoretical V-belt length of 1115 mm, roller mass of approximately 5.55 kg, and shaft torsional shear stress of 2.51 N/mm². These results provide a technical basis for prototype development; however, operational feasibility remains unconfirmed because combined loading, vibration, surface roughness, productivity, and actual power consumption have not been experimentally evaluated.

Keywords: *AutoCAD, Belt Sander, Machine Design, Transmission System, Wood Sanding Machine.*

A. INTRODUCTION

Wood processing is an important part of the production of furniture, frames, doors, interior components, and various craft products. Surface quality is one of the determinants of the success of the final stage because uneven surfaces, coarse fibers, or cutting marks can affect painting, coating, bonding, and the application of protective materials (Bekhta et al., 2022; Yu et al., 2023). Sanding is used to level surfaces, remove coarse fibers, and create surface conditions that are better prepared for finishing processes (Bekhta et al., 2022). In small workshops and industries, this work is still often performed using hand sandpaper or simple equipment. Although manual methods are flexible and do not require substantial investment, they require relatively high amounts of time and labor and depend heavily on operator skill. Variations in hand pressure, inconsistent movement direction, and differences in contact duration can result in less consistent sanding outcomes (Bembenek, 2022).

A belt-sander system offers continuous abrasive motion by using a sanding belt that rotates around a drive roller and an idler roller. The drive roller receives power from the motor through a transmission system, while the idler roller maintains the belt path and tension (Matejić et al., 2022). More stable contact between the belt and workpiece has the potential to accelerate material removal and improve process consistency compared with manual sanding. However, designing a belt sander involves more than simply determining the frame structure and installing a motor. Rotational speed, torque, roller diameter, belt linear speed, pulley alignment, V-belt tension, shaft strength, bearing selection, frame stability, and operator safety are interrelated. Errors in one component can lead to slippage, belt misalignment, vibration, uneven wear, or component failure (Wang et al., 2022).

Previous studies have discussed belt-sander prototypes, table portability, surface roughness characteristics, sanding efficiency, abrasive-belt wear, and transmission-system behavior (Wu et al., 2022; Wang et al., 2022). However, there remains a need for an integrated design that specifically establishes the specifications of the motor, pulleys, V-belt, rollers, shaft, bearings, and frame, along with engineering drawings for small workshops or industries. The gap between the expected and existing conditions lies in the need for a simple machine that can be constructed using commonly available components, while manual sanding remains dominant and existing designs do not always provide an integrated calculation basis for each component. The practical novelty of this study does not lie in the discovery of a new sanding principle, but rather in the integration of a mechanical configuration adapted to small-scale requirements and translated into AutoCAD design and working drawings.

Based on this gap, this study aimed to design a belt-sander wood sanding machine for small workshops and industries, establish the specifications of its main components, perform basic engineering calculations for the driving and supporting elements, and produce design and working drawings using AutoCAD. The study was limited to the theoretical design stage and did not include prototype fabrication or testing. Therefore, the results are positioned as an initial basis for further development rather than evidence that the machine has met all operational performance and safety indicators.

B. LITERATURE REVIEW

Previous studies have shown that both machine characteristics and abrasive systems determine sanding performance. Setiawan, Pramono, and Waluyo (2023) designed a belt-sander machine using a 1 HP motor with a rotational speed of 2800 rpm and a 2:1 pulley ratio system. Their study confirmed that the pulley ratio has a direct effect on the working speed. Rizqullah et al. (2024) developed a belt sander with a portable table and incorporated mobility, ease of movement, and work-position adjustment as part of the design criteria. These two studies demonstrate that a belt-sander machine for workshop-scale applications must balance mechanical performance with ease of use and practical construction.

From the process perspective, Sydor et al. (2021) showed that machine sanding efficiency is influenced by wood species and abrasive-belt grit size. Hardwood and softwood do not respond identically to abrasives; therefore, belt speed and grit selection need to be adjusted to the material being processed. Adamčík et al. (2024) compared the surface roughness of beech wood after sanding using an eccentric sander and a belt sander. Their findings showed that a belt sander, particularly when using coarse grit, can leave more pronounced scratch marks. This finding is important because a high material removal rate does not necessarily correspond to the best surface quality. A machine design should provide stable belt movement and allow adjustment of operating procedures rather than simply pursuing high rotational speed.

Abrasive-belt wear and failure are also factors that cannot be overlooked. Zhang et al. (2021) explained that belt wear during medium-density fiberboard sanding can occur through abrasive grain wear, grain fracture, and grain detachment from the backing layer. Du et al. (2022) added that the clogging of wood particles in the spaces between abrasive grains can reduce material-removal capability. Li et al. (2024) showed that the shape and characteristics of abrasive grains affect the stability of material removal and surface quality. The implications for machine design are that the rollers must be capable of driving the belt without excessive slip, the belt path must be maintained, and the belt replacement mechanism should be easy to operate because the belt is a consumable component.

In the transmission system, changes in loading conditions can affect slip, vibration, and the operating condition of other components. Mascenik and Coranic (2024) discussed the effect of changes in loading conditions on belt transmission and the operating condition of the system. Tauvana, Syafrizal, and Ramadhan (2026) showed that asymmetric load distribution in V-belt and pulley systems can affect stability and slip, although their study focused on a belt conveyor. The principle remains relevant because a sanding machine also uses a flexible transmission system that requires proper shaft alignment and belt tension. Tjiptady et al. (2023) demonstrated that variations in roller mass and V-belt width are associated with the torque, power, and speed of the system. Therefore, roller mass, pulley ratio, and belt dimensions need to be treated as interrelated design parameters.

C. METHOD

This study used an engineering design approach. The subject in the context of this study was not human respondents, but rather the design object, namely a belt-sander wood sanding machine. The research activities focused on translating work requirements into a machine configuration, selecting components, performing basic analytical calculations, and documenting engineering drawings. The study was conducted as a design study at the Mechanical Engineering Workshop of Manado State Polytechnic from March to June 2026. The final outputs of the study were a design model, component specifications, theoretical calculation results, and working drawings that can be used as an initial reference for prototype fabrication.

The design data were obtained through a literature review, examination of previous studies, identification of workshop work requirements, assessment of commonly available components, and determination of initial dimensions. The instruments used included AutoCAD software for developing two- and three-dimensional models, component catalog data for determining appropriate shaft and bearing dimensions, and machine-element equations for calculating rotational speed, torque, belt speed, V-belt length, tangential force, roller mass, and shaft shear stress. The study did not use surface roughness testers, vibration meters, wattmeters, or material testing equipment because the prototype had not yet been fabricated.

The design procedure began with identifying the problems associated with manual sanding and the machine requirements for workshop-scale applications. The next stage involved a literature review of belt sanders, sanding process characteristics, pulley and V-belt transmissions, rollers, shafts, bearings, and frames. Based on the results of the review, an initial design concept was developed, machine dimensions and component specifications were determined, and engineering calculations were then performed. The calculation results were used to evaluate the consistency between motor power, transmission ratio, roller speed, and component dimensions. The concept was then translated into AutoCAD design drawings. If the component arrangement or dimensions were found to be unsuitable, the design was revised before being finalized. The overall procedure is presented in Figure 1.

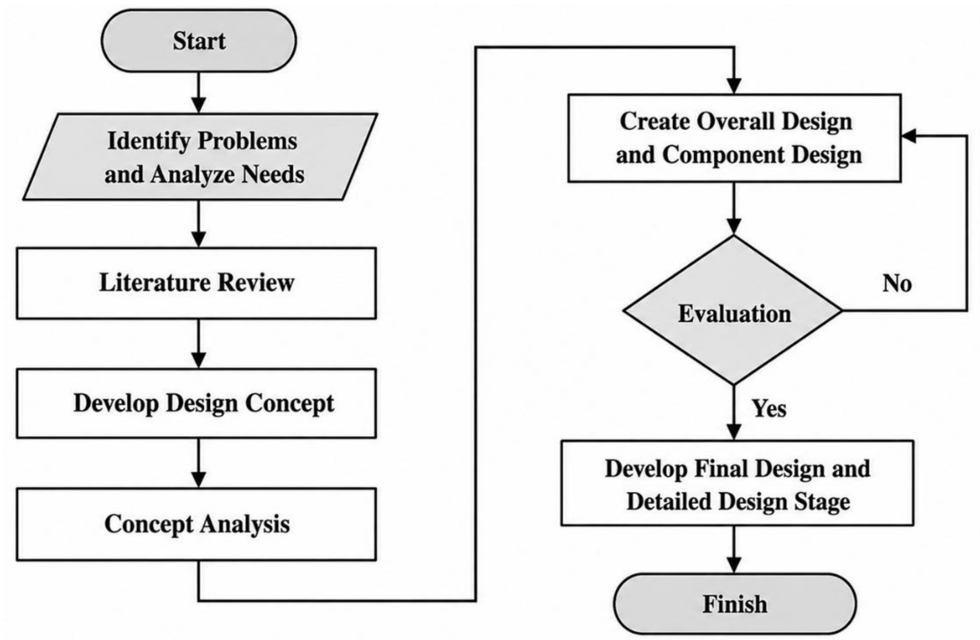

Figure 1. Design Process Flow of the Wood Sanding Machine

The calculations began by converting the motor rotational speed into angular velocity. The motor angular velocity was calculated using the following equation:

$$\omega = 2\pi n / 60$$

where ω is the angular velocity in rad/s and n is the motor speed in rpm. Motor torque was determined from the relationship between power and angular velocity:

$$T = P / \omega$$

The drive-roller speed was calculated based on the pulley diameter ratio while neglecting slip:

$$n_2 = n_1(d_1 / d_2)$$

The theoretical V-belt length for an open transmission was calculated using the diameters of the large pulley D, small pulley d, and center distance C:

$$L = 2C + (\pi/2)(D + d) + (D - d)^2 / (4C)$$

The linear speed of the sanding belt was obtained from the roller diameter and drive-roller speed:

$$v = \pi D n / 60$$

The theoretical roller torque was determined from the pulley diameter ratio. The tangential force was calculated using $F = T/r$. The torsional shear stress in the solid shaft was calculated using $\tau = 16T/(\pi d^3)$. The mass of the roller pipe was calculated from the volume of the hollow cylinder and the material density, while the mass of the rubber layer was calculated from the difference between the volumes of the outer and inner cylinders. All results were analyzed descriptively by comparing the relationships among parameters and previous designs. The analysis did not include transmission efficiency, belt tension force, shaft bending load, bearing life, frame deflection, or actual sanding load. These limitations were applied to ensure that the conclusions remained consistent with the data actually available.

D. RESULT AND DISCUSSION

1. Design Concept and Configuration

The resulting design uses a horizontal belt-sander configuration with two rollers positioned at the top of the frame. The sanding belt forms an elongated working surface, allowing the workpiece to be guided along the belt surface. The electric motor is positioned at the bottom of the frame to lower the machine's center of mass and facilitate the arrangement of the transmission system. Motor rotation is transmitted through the driving pulley and V-belt to the pulley mounted on the drive-roller shaft. The idler roller serves as a belt support and guide, while the two rollers must be properly aligned to prevent the belt from moving laterally. The general configuration of the design is shown in Figure 2.

The overall machine dimensions are 1000 mm in length, 500 mm in width, and 750 mm in height. These dimensions result in a freestanding machine that can be placed in a small workshop without requiring a special foundation. The frame uses 40 × 40 × 2 mm hollow steel with horizontal reinforcements. The hollow steel was selected based on its ease of cutting and welding, material availability, and closed cross-sectional shape, which provides greater stiffness than flat bars with a comparable mass. Nevertheless, this study did not calculate frame deflection or the dynamic response caused by roller imbalance. Therefore, the frame dimensions represent an initial design decision rather than the result of comprehensive structural verification.

The motor mount is designed using a 10 mm-thick steel plate and 50 × 50 × 5 mm angle steel. The motor mounting holes should be elongated to allow the motor position to be adjusted when setting the V-belt tension. This adjustment feature is important because the pulley center distance and belt tension affect slip and the radial load on the shaft. A design using only fixed round holes can still be assembled, but it would make it difficult to correct belt-length tolerances and make adjustments after the belt has elongated. Therefore, the adjustment system is a functional element rather than merely an additional construction feature.

The rollers use ST42 carbon-steel pipes with an outer diameter of 100 mm, a thickness of 4 mm, and a length of 460 mm. The roller surfaces are covered with 8 mm-thick rubber lagging to increase the coefficient of friction and reduce the tendency for slip between the roller and sanding belt. The shaft uses S45C steel with a diameter of 25 mm and a length of 520 mm. UCP205 bearings were selected because their bore diameter matches the 25 mm shaft, while their pillow-block configuration facilitates installation on the frame. Diameter compatibility alone is not sufficient to establish bearing life; the dynamic and static capacities must be evaluated once the belt tension force and sanding load are known.

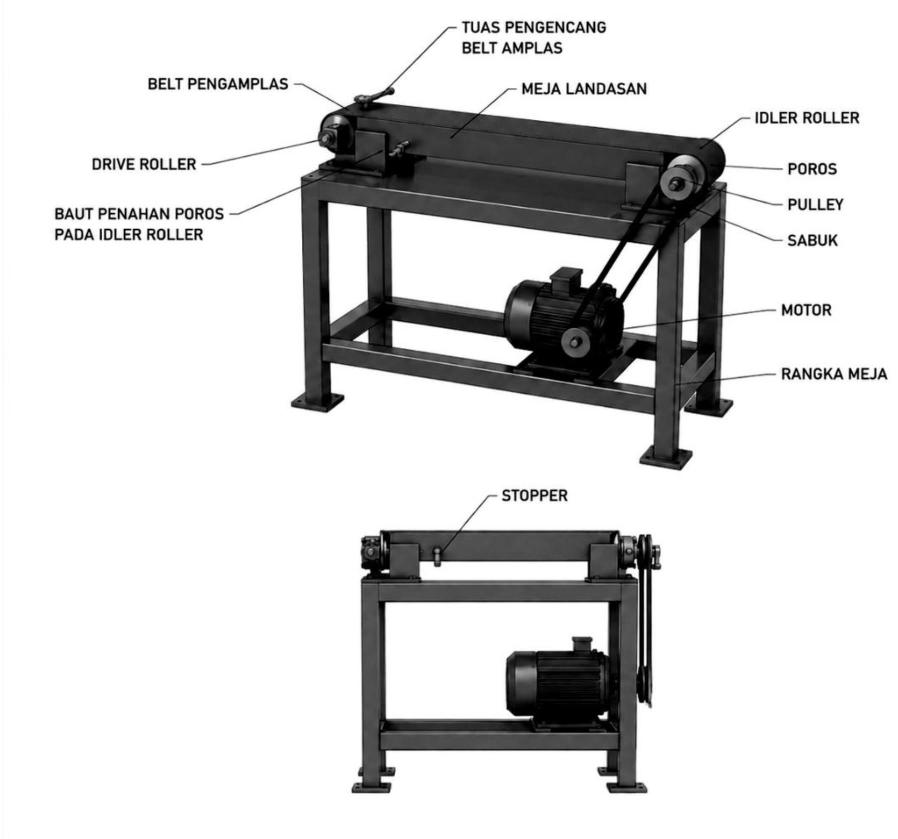

Figure 2. General Configuration of the Wood Sanding Machine

The main design specifications are summarized in Table 1 below:

Table 1. Main Specifications of the Machine Design

Group	Parameter	Specification
System	Machine type	Belt sander for wood sanding
Drive	Electric motor	1 HP / 0,746 kW; 1390 rpm
Transmission	Driving pulley	Diameter 80 mm
Transmission	Driving pulley	Diameter 120 mm
Transmission	Belt	A-type V-belt; one belt
Roller	Dimensions	Ø100 mm × 460 mm length; 4 mm pipe thickness
Roller	Material and coating	ST42 carbon-steel pipe; 8 mm rubber lagging
Shaft	Material and dimensions	S45C steel; Ø25 mm × 520 mm length
Bearing	Type	UCP205; 25 mm bore diameter
Frame	Material	40 × 40 × 2 mm hollow steel
Frame	Overall dimensions	1000 × 500 × 750 mm
Motor mount	Material	10 mm plate and 50 × 50 × 5 mm angle steel
Design	Software	AutoCAD

2. Drive and Transmission System Analysis

The selected electric motor has a nominal power of 0.746 kW and a rotational speed of 1390 rpm. Its angular velocity is 145.49 rad/s. By dividing the power of 746 W by the angular velocity, a motor torque of 5.13 N·m was obtained. This value represents the theoretical torque based on the nominal power and does not account for electrical or mechanical losses. In actual operation, the power available at the shaft may be lower due to motor efficiency, bearing friction, belt bending, and slip. Because this study did not have component efficiency data, the use of the ideal value must be explicitly stated so that the result is not interpreted as the actual capability of the machine.

The 80 mm-diameter motor pulley and 120 mm-diameter drive-roller pulley produced a reduction ratio of 1.5. The roller speed was calculated as 926.67 rpm. This speed reduction increased the theoretical torque from 5.13 N·m to approximately 7.70 N·m at the drive roller. This relationship is consistent with the principle of ideal power conservation: a reduction in angular speed is accompanied by an increase in torque. This ratio is more moderate than designs using a 2800 rpm motor because an excessively high roller speed can result in high belt speed, increase the risk of heat generation, and accelerate abrasive-belt wear. Conversely, an excessively low speed can reduce the material removal rate. The 80:120 ratio represents an initial compromise, but the optimum operating point still needs to be determined through testing with different wood types and grits.

With a pulley center distance of 400 mm, the theoretical V-belt length was obtained as 1115 mm. This value should be understood as a geometric length. During fabrication, the belt cannot be ordered based solely on the theoretical value without considering the belt numbering system, pitch length, outside length, manufacturer tolerances, and the adjustment range of the motor mount. Therefore, an adjustable motor mount is required to accommodate the nearest standard belt length. This statement also indicates the limitation of the assumed 400 mm center distance: the value represents a layout decision rather than an optimization based on commercially available belt sizes.

The linear speed of the sanding belt was calculated from the roller diameter of 0.1 m and a speed of 926.67 rpm, resulting in 4.85 m/s. This value is higher than the design by Putra, Yetri, and Maimuzar (2018), which, based on the comparative thesis data, had a belt speed of 0.38 m/s. This difference does not automatically demonstrate that the new design is better. A higher speed can increase the material removal rate, but it can also increase heat generation, accelerate belt clogging, and produce deeper scratches if the grit or contact pressure is inappropriate. The findings of Sydor et al. (2021) and Adamčík et al. (2024) support the need to evaluate speed together with wood type, grit, and surface quality rather than as a single indicator.

The theoretical tangential force at the roller surface was calculated from a torque of 7.70 N·m and a radius of 0.05 m, resulting in 154 N. This value represents the ideal circumferential force that can be derived from the roller torque. However, this force is not the direct sanding force acting on the workpiece. The actual contact force is influenced by belt tension, contact area, coefficient of friction, operator-applied pressure, rubber-lagging elasticity, and transmission efficiency. Equating 154 N with the cutting or pressing force would be a conceptual error. In this article, the value is used to understand the scale of the force at the roller and as an initial basis for further analysis, rather than to indicate sanding capacity.

The calculation results for the drive and transmission systems are summarized in Table 2. The mathematical consistency among the results is satisfactory: the pulley ratio reduces the speed to two-thirds of the motor speed, increases the torque to one and a half times the motor torque, and produces a belt speed consistent with the roller diameter. However, mathematical consistency differs from functional validation. Without measurements of slip, motor current, temperature rise, and actual speed, these values remain predictive.

Table 2. Theoretical Calculation Results of the Design

Parameter	Result	Description
Motor angular velocity	145,49 rad/s	From 1390 rpm
Motor torque	5,13 N·m	Based on nominal power of 746 W
Drive-roller speed	926,67 rpm	Pulley ratio of 80:120
V-belt length	1115 mm	Theoretical value for C = 400 mm
Drive-roller torque	7,70 N·m	Ideal, transmission losses neglected
Sanding-belt speed	4,85 m/s	Roller Ø100 mm
Roller tangential force	154 N	T/r with r = 0.05 m
Shaft shear stress	2,51 N/mm²	Due to torque only
Total mass of one roller	≈5,55 kg	4.36 kg pipe + 1.19 kg rubber

3. Analysis of the Roller, Shaft, and Bearings

The mass of the roller pipe was calculated using an outer diameter of 100 mm, an inner diameter of 92 mm, a length of 460 mm, and a steel density of 7850 kg/m³. The volume of the hollow cylinder resulted in a mass of approximately 4.36 kg. The 8 mm-thick rubber lagging was calculated for a coating length of 400 mm with a rubber density of 1100 kg/m³, resulting in a mass of approximately 1.19 kg. The total mass of one roller was therefore approximately 5.55 kg. The difference between the 460 mm pipe length and the 400 mm rubber coating length leaves an area on both sides for connection to the roller end components or assembly tolerances. This dimension needs to be confirmed in the working drawings to avoid ambiguity during manufacturing.

Roller mass affects the moment of inertia and the load on the bearings. A heavier roller tends to maintain more stable rotation after reaching operating speed, but requires greater acceleration torque and increases the forces caused by imbalance. Tjiptady et al. (2023) demonstrated the relationship between roller and V-belt parameters and the torque and speed of the system. In this design, the calculation only covers static mass and does not include the moment of inertia or acceleration time. Because the motor was selected based on nominal power rather than calculations of acceleration requirements and sanding loads, its starting capability should be tested on the prototype. Even a small imbalance in a roller rotating at 926.67 rpm can generate vibration that is not apparent in static analysis.

The 25 mm-diameter S45C shaft is subjected to a theoretical torque of 7.70 N·m. The torsional shear stress was calculated as 2.51 N/mm². This value is relatively low compared with the typical capacity of shaft steel, but the conclusion that the shaft is safe should not be based solely on torsional stress. The shaft also carries the roller weight, radial force from V-belt tension, forces resulting from sanding-belt contact, and possible impact loads when the workpiece is pressed against the belt. These loads generate bending moments that need to be combined with torque. In addition, keyways, changes in diameter, roller connections, and stress concentrations can reduce the effective strength. Therefore, the value of 2.51 N/mm² only indicates that the component is not critical under nominal torsion considered separately; it does not constitute a complete shaft assessment.

The UCP205 bearing is compatible with the 25 mm shaft diameter and has a housing that facilitates position adjustment on the frame. This selection is rational in terms of geometric compatibility and ease of maintenance. However, the study did not calculate the equivalent load, L10 life, limiting speed, or the effects of misalignment. The radial load on the bearing depends on the tension of the V-belt and sanding belt, while these data are not yet available. Therefore, the defensible statement is that the UCP205 is dimensionally compatible and suitable as an initial candidate, rather than that its service life or capacity has been verified.

Rubber lagging was selected to increase traction. The rubber layer can help reduce slip, but the roller surface geometry also affects belt tracking. A completely cylindrical roller requires high alignment accuracy, whereas a slight crown profile is often used to help the belt return to the center. The thesis has not yet specified the crown profile or the idler adjustment mechanism in detail. This issue needs to be resolved before prototype fabrication because belt tracking failure is an operational risk and can damage the belt edges. The studies by Li et al. (2024), Zhang et al. (2021), and Du et al. (2022) also indicate that movement stability and abrasive-belt condition affect material removal and belt service life.

4. Design Drawings and Manufacturing Readiness

AutoCAD was used to create three-dimensional models and working drawings of the components. The drawing documents include the machine assembly, frame, motor mount, drive roller, idler roller, shaft, and transmission system. The overall drawing shows the relationships among the components, while the working drawings provide basic dimensions for cutting, drilling, welding, and assembly. One sheet of the design drawings is shown in Figure 3. The use of AutoCAD is consistent with the objective of the study because the focus is on geometric documentation rather than stress simulation.

The availability of working drawings does not automatically guarantee full manufacturing readiness. A production-ready drawing should specify dimensional tolerances, alignment tolerances, weld types and sizes, shaft surface roughness, fits between the shaft and bearing, pulley key details, material for each component, and the idler and motor adjustment mechanisms. The drawings in the thesis provide the main shapes and dimensions, but some of these details still need to be clarified before being submitted to the workshop. This is important because small tolerances in the positions of the bearings or rollers can cause unstable belt tracking.

Safety aspects must also be incorporated into the production drawings. Exposed pulleys and V-belts can catch the operator's clothing or body parts, while the moving sanding belt can eject workpieces and generate wood dust. Further design development should include transmission guards, belt-side guards, an emergency stop button, an easily accessible switch, and a dust-collection system. Adding these components will change the machine mass, layout, and space requirements, so they should preferably be incorporated before the first prototype is fabricated rather than after the machine has been assembled.

Figure 3. Overall Machine Design Drawing Using AutoCAD

5. Comparison with Previous Designs

A comparison with the mechanical belt-sanding machine developed by Putra et al. (2018) was conducted to demonstrate differences in specifications and the depth of analysis. The previous design used a ¼ HP motor, whereas the present design uses a 1 HP motor. The previous motor speed was reported as 2800 rpm, with a pulley speed of 1521.7 rpm, while the present design uses a 1390 rpm motor and produces a roller speed of 926.67 rpm. The belt speed of the present design is 4.85 m/s, which is higher than the comparative value of 0.38 m/s. In addition, the present design calculates motor torque, roller torque, tangential force, shaft shear stress, and roller mass, which were not reported in the comparative data.

The comparison demonstrates the broader scope of the calculation documentation, but it cannot be used to claim superior performance. The design by Putra et al. (2018) involved machine development and fabrication, whereas the present study stops at the design stage. A machine with greater power is not necessarily more efficient, and a higher belt speed does not necessarily produce a better surface. Without testing the same wood types, grit, pressure, and sanding duration, claims of superiority would go beyond the available evidence. Therefore, Table 3 is presented as a comparison of configurations and theoretical parameters rather than a performance ranking.

Differences in the design approach are also evident in the design objectives. The present design emphasizes the use of standard components, a 25 mm shaft, UCP205 bearings, ST42 rollers, and AutoCAD working drawings for workshop-scale applications. Its main added value is the traceability of the relationship between specifications and calculation results. Conversely, its main limitation is the absence of experimental evidence. The more appropriate scientific position is that this design expands the technical basis for the prototype stage rather than replacing the testing conducted in machine development studies.

Table 3. Comparison of the Design with the Study by Putra et al. (2018)

Aspect	Putra et al. (2018)	This Design
Motor power	¼ HP	1 HP / 0,746 kW
Motor speed	2800 rpm	1390 rpm
Pulley/roller speed	1521,7 rpm	926,67 rpm
Belt speed	0,38 m/s	4,85 m/s
Belt length	1051,69 mm	1115 mm
Motor torque	Not reported	5,13 N·m
Roller torque	Not reported	7,70 N·m
Tangential force	Not reported	154 N
Shaft shear stress	Not reported	2,51 N/mm²
Roller mass	Not reported	5,55 kg
Bearing	Not reported in the comparison	UCP205

6. Evaluation of Design Feasibility and Limitations

Internally, the design demonstrates logical relationships among the parameters. The 1390 rpm motor is reduced by the 80 and 120 mm pulleys to 926.67 rpm; torque increases according to the ideal ratio; the 100 mm roller produces a belt speed of 4.85 m/s; and the 25 mm shaft experiences relatively low nominal torsional stress. The main components are also geometrically compatible: the 25 mm shaft matches the UCP205 bearing, the 460 mm roller can be accommodated within the 500 mm-wide frame with mount adjustment, and the motor is positioned to allow V-belt transmission. Based on this consistency, the design can be considered feasible as an initial basis for prototype fabrication.

However, the term feasible must be qualified. The study has not determined the actual sanding force; therefore, the motor power requirement was not calculated from the process load. The 1 HP power was selected first, and the torque was then derived from the motor specifications. This approach is useful for predicting system output, but it does not demonstrate that 1 HP is the minimum or optimum power. Prototype testing should measure current, input power, the reduction in speed under load, and motor temperature. If the speed drops sharply or the motor operates near overload for extended periods, the transmission ratio or motor power should be reconsidered.

The shaft analysis only considers torque. In practice, V-belt tension creates a radial load on the pulley side, roller weight produces bending, and workpiece pressure adds load to the working surface. The combination of bending and torsion may represent a more critical design condition than torsion alone. Similarly, the bearing was selected based on diameter without a service-life calculation, while the frame was selected based on dimensions and construction experience without deflection analysis. The conclusions should reflect these limitations so that readers do not equate the basic calculation results with comprehensive safety verification.

Sanding performance cannot yet be evaluated because there are no data on surface roughness, processing time, production capacity, actual energy consumption, belt temperature, noise, vibration, or tracking stability. The studies by Sydor et al. (2021) and Adamčík et al. (2024) show that the quality of the results is strongly influenced by wood type and grit. Therefore, the prototype should be tested using several wood types representing different levels of hardness and several grits appropriate for different sanding stages. Pressure should be controlled so that the comparison is not dominated by operator-applied force.

Dust and safety aspects are design requirements that have not yet been calculated. Wood dust can affect health, contaminate bearings, and clog the abrasive belt. A dust-extraction system with a duct positioned near the contact zone should be considered. Guards for the pulleys, V-belt, and sanding-belt sides should prevent accidental contact without obstructing belt replacement. An emergency stop button should be positioned within the operator's reach. Adding these features may increase cost and complexity, but ignoring them would make an apparently simple design unsuitable for actual operation.

Considering its strengths and limitations, the contribution of this study lies in the development of a structured and transparent mechanical design. Each major value can be traced to a specification or equation, and the AutoCAD drawings provide a basis for communication between the designer and the workshop. This contribution is relevant to design research at the initial stage. The next stage should shift the focus from theoretical consistency toward validation: prototype fabrication, verification of alignment and roller balance, measurement of actual speed, load testing, surface roughness testing, vibration and noise measurements, and safety evaluation.

E. CONCLUSION

This study produced a theoretical design of a belt-sander wood sanding machine for small workshops and industries with dimensions of 1000 × 500 × 750 mm. The machine uses a 1 HP motor operating at 1390 rpm, 80 and 120 mm pulley transmission, an A-type V-belt, an ST42 roller measuring Ø100 × 460 mm with 8 mm rubber lagging, a Ø25 mm S45C shaft, UCP205 bearings, and a 40 × 40 × 2 mm hollow-steel frame. The calculations resulted in a drive-roller speed of 926.67 rpm, motor torque of 5.13 N·m, roller torque of 7.70 N·m, belt speed of 4.85 m/s, tangential force of 154 N, theoretical V-belt length of 1115 mm, roller mass of 5.55 kg, and shaft shear stress of 2.51 N/mm². These results are consistent as an initial basis for prototype fabrication and AutoCAD working drawings, but they do not demonstrate operational performance because the actual sanding load, combined shaft bending and torsion, bearing life, frame deflection, surface roughness, energy consumption, belt tracking, vibration, noise, and safety have not been tested. The next stage should refine the manufacturing and safety details, fabricate the prototype, and conduct controlled testing.

REFERENCES

Adamčík, L., Dzurenda, L., Banski, A., & Kminiak, R. (2024). Comparison of surface roughness of beech wood after sanding with an eccentric and belt sander. *Forests, 15*(1), 45. https://doi.org/10.3390/f15010045

Bekhta, P., Lis, B., Krystofiak, T., & Bekhta, N. (2022). Surface roughness of varnished wood pre-treated using sanding and thermal compression. *Forests, 13*(5), 777.

Bembenek, M. (2022). Researches on influence of wood sanding direction on wood gluing. *Journal of the Indian Academy of Wood Science, 19*(2), 103-109.

Du, Y., Sun, X., Luo, B., Li, L., & Liu, H. (2022). Research on failure mechanism of abrasive belt and effect on sanding of medium-density fiberboard (MDF). *Coatings, 12*(5), 621. https://doi.org/10.3390/coatings12050621

Li, C., Du, Y., Luo, B., Li, L., & Liu, H. (2024). Sanding performance and wear mechanism of precision-shaped abrasive belts for medium-density fiberboard. *Forests, 15*(11), 1934. https://doi.org/10.3390/f15111934

Matejic, M., Matejic, M., Živić, J., & Ivanović, L. (2022). *Design and Testing of Abrasive Belt Grinder*.

Mascenik, J., & Coranic, T. (2024). The influence of changing belt loading conditions on the operational condition of the belt transmission. *Actuators, 13*(12), 506. https://doi.org/10.3390/act13120506

Putra, A. I., Yetri, Y., & Maimuzar. (2018). Rancang bangun mesin amplas dengan sistem mekanis belt. *Jurnal Teknik Mesin, 11*(2), 63–69. https://doi.org/10.30630/jtm.11.2.169

Rizqullah, H. Q., Ardiza, R., Alvin, Pangestu, R. D., Firmansyah, F. A., & Lestari, W. D. (2024). Rancang bangun mesin belt sander dengan meja portabel. *TESME, 1*(1), 122–128.

Setiawan, I. H., Pramono, G. E., & Waluyo, R. (2023). Rancang bangun mesin belt sander. *ALMIKANIKA, 5*(2), 46–55. https://doi.org/10.32832/almikanika.v5i2.13890

Sydor, M., Mirski, R., Stuper-Szablewska, K., & Rogoziński, T. (2021). Efficiency of machine sanding of wood. *Applied Sciences, 11*(6), 2860. https://doi.org/10.3390/app11062860

Tauvana, A. I., Syafrizal, & Ramadhan, G. (2026). The influence of asymmetric load distribution on V-belt and pulley transmission in belt conveyor systems. *Jurnal Rekayasa Mesin, 21*(1). https://doi.org/10.32497/jrm.v21i1.7515

Tjiptady, B. C., Rahman, R. Z., Rohman, M., Nugroho, M. H., & Pradani, Y. F. (2023). Pengaruh variasi torsi roller dan lebar V-belt terhadap top speed mesin. *Metrotech: Journal of Mechanical and Electrical Technology, 2*(3), 136–143. https://doi.org/10.33379/metrotech.v2i3.3378

Wang, Y., Huang, X., Ren, X., Chai, Z., & Chen, X. (2022). In-process belt-image-based material removal rate monitoring for abrasive belt grinding using CatBoost algorithm. *The International Journal of Advanced Manufacturing Technology, 123*(7), 2575-2591.

Wu, X., Niu, H., Li, X. J., & Wu, Y. (2022). Research on GA-BP neural network model of surface roughness in air drum sanding process for poplar. *European Journal of Wood and Wood Products, 80*(2), 477-487.

Yu, Q., Pan, X., Yang, Z., Zhang, L., & Cao, J. (2023). Effects of the surface roughness of six wood species for furniture production on the wettability and bonding quality of coating. *Forests, 14*(5), 996.

Zhang, J., Yang, Y., Luo, B., Liu, H., & Li, L. (2021). Research on wear characteristics of abrasive belt and the effect on material removal during sanding of medium density fiberboard (MDF). *European Journal of Wood and Wood Products, 79*, 1563–1576. https://doi.org/10.1007/s00107-021-01718-x